

POSSIBLE ORIGIN OF RADIO EMISSION FROM NONTHERMAL ELECTRONS IN HOT ACCRETION FLOWS FOR LOW-LUMINOSITY ACTIVE GALACTIC NUCLEI

HU LIU AND QINGWEN WU^{*}
printed at February 26, 2018, accepted by ApJ

ABSTRACT

The two components of radio emission, above and below 86 GHz respectively, from the Galactic center source—Sgr A* can be naturally explained by the hybrid of thermal and nonthermal electrons in hot accretion flows (e.g., radiatively inefficient accretion flow, RIAF, e.g., Yuan et al. 2003). We further apply this model to a sample of nearby low-luminosity active galactic nuclei (LLAGNs), which are also believed to be powered by the RIAF. We selected the LLAGNs with only compact radio cores according to the high-resolution radio observations, and the sources observed with jets or jet-like features are excluded. We find that the radio emission of LLAGNs is severely underpredicted by pure RIAF model, and can be naturally explained by the RIAF model with a hybrid electron population consisting of both thermal and nonthermal particles. Our model can roughly reproduce the observed anti-correlation between the mass-corrected radio loudness and Eddington ratio for the LLAGNs in our sample. We further model the spectral energy distributions of each source in our sample, and find that roughly all sources can be well fitted if a small fraction of the steady state electron energy is ejected into the nonthermal electrons. The size of radio emission region of our model is around several thousand gravitational radii, which is also roughly consistent with the recent high-resolution VLBI observations for some nearby LLAGNs.

Subject headings: accretion, accretion disks-black hole physics-galaxies: active-radiation mechanisms: nonthermal

1. INTRODUCTION

Active galactic nuclei (AGNs) produce enormous luminosities in extremely compact volumes. It was found some local galaxies show similarities to those of bright AGNs, but with relatively weaker broad-line emission and multiwavelength radiative cores (e.g., Ho et al. 1997, 2001; Falcke & Markoff 2000; Nagar et al. 2002; Maoz 2007). These low-luminosity active galactic nuclei (LLAGNs) are very common in the local universe, which may be the scaled-down luminosity version of bright AGNs (see Ho 2008, for a recent review). Actually, the AGN may only spend a small fraction of its lifetime in the highly luminous, QSO-like phase, and much more time is spent in a weakly accreting state (LLAGNs or normal galaxies, e.g., Hopkins & Hernquist 2006). Both bright AGNs and LLAGNs are believed to be powered by the matter falling onto a super massive black hole (BH). The observational properties of LLAGNs are quite different from those of bright QSOs, which are thought to be driven by different accretion modes. The optical/UV bumps observed in QSOs can be naturally interpreted as multi-temperature blackbody emission from a cold, optically thick, and geometrically thin standard disk (SSD, Shakura & Sunyaev 1973). However, most of LLAGNs lack the evident optical/UV bump as that of bright AGNs. The possible physical reason is that the standard thin accretion disk is absent in these LLAGNs. A hot, optically thin, geometrically thick radiatively inefficient accretion flow model has been developed in the last several decades (RIAF, an ‘updated’ version of the original advection dominated accretion flow model, ADAF; e.g., Ichimaru 1977; Narayan & Yi 1994, 1995; Abramowicz et al. 1995; see Kato et al. 2008; Narayan & McClintock 2008; and Yuan & Narayan

2013 for reviews). The RIAF model can successfully explain most observational features of nearby LLAGNs (e.g., Quataert et al. 1999; Cao & Rawlings 2004; Nemmen et al. 2006; Wu et al. 2007; Wu & Gu 2008; Gu & Cao 2009; Yuan et al. 2009a; Yuan et al. 2009b; Xu & Cao 2009; Ho 2009; Cao 2010; Yu et al. 2011; Nemmen et al. 2012; see Yuan 2007 and Ho 2008 for recent reviews).

The AGNs are traditionally divided into radio loud (RL) and radio quiet (RQ), and the origin for this dichotomy is still a matter of debate. The distinction between the RL and RQ objects is normally based on a radio-loudness parameter, which was defined as the ratio of the monochromatic flux density at 5 GHz and optical B band at 4400 Å ($R_o = F_{5\text{ GHz}}/F_B$). The loudness $R_o = 10$ is usually taken as the division between RQ and RL AGNs (particularly in QSO studies, e.g., Kellermann et al. 1994). Terashima & Wilson (2003) introduced a new definition of the radio loudness parameter by comparing the 5 GHz radio luminosity to the 2-10 keV luminosity, $R_X = L_{5\text{ GHz}}/L_{2-10\text{ keV}}$, and proposed that $\log R_X = -4.5$ would be the barrier separating RL and RQ AGNs, which roughly corresponding to $R_o = 10$. The use of X-ray luminosity with respect the optical one should largely avoid extinction problems which normally occur in the optical band. However, most of the traditionally RQ LLAGNs become RL according to the criterion $R_o = 10$ or $\log R_X = -4.5$ if using their nuclear emission at radio and optical/X-ray waveband (e.g., Ho 2002; Panessa et al. 2006). Panessa et al. (2006) redefined the boundary for the RL and RQ LLAGNs as $\log R_X \sim -2.8$ based on a sample of low-luminosity Seyferts and Fanaroff-Riley type I radio galaxies (FR Is). In the last decade, there is great progress in estimating the BH mass in both normal galaxies and AGNs (e.g., Gebhardt et al. 2000; Kaspi et al.

¹ School of Physics, Huazhong University of Science and Technology, Wuhan 430074, China;

* Corresponding author, Email: qwwu@hust.edu.cn

2005). The measurements of BH mass help us to further understand the issue of radio loudness. Ho (2002) found that the loudness parameter increases with decreasing of the Eddington ratio. Sikora et al. (2007) investigated the radio loudness of a total 199 sources which include broad-line radio galaxies (BLRGs), RL QSOs, Seyferts, low-ionization nuclear emission-line region galaxies (LINERs), FR Is, and Palomar-Green QSOs (PGQs), and found that there are two distinct, approximately parallel tracks on radio-loudness–Eddington-ratio plane. They further proposed a quantitative definition for the radio-loudness parameter that is dependent on the Eddington ratio (see their equation 5), where the RL sources include BLRGs, RL QSOs, FR Is, while RQ sources comprise Seyferts, LINERs and PGQs (hereafter we use this criteria to distinguish the RL/RQ).

The radio emission of RL AGNs is believed to originate in the relativistic jets, where many large-scale radio jets have been observed directly. Compared with RL AGNs, the origin of nuclear radio emission from RQ objects is still not well understood, since that RQ AGNs are much fainter radio sources, and most of them only show a compact radio core. The radio variability of RQ QSOs confined the radio emission to $\lesssim 0.1$ pc (e.g., Barvainis et al. 2005), and the high-resolution VLBI observations show that the region of the radio emission in RQ LLAGNs should be $\lesssim 10^{-4}$ to $\lesssim 10^{-2}$ pc (e.g., Ho & Ulvestad 2001; Nagar et al. 2002; Giroletti & Panessa 2009). Several possibilities have been proposed to explain the radio emission in these RQ AGNs. The first explanation is that RQ AGNs are scaled-down version of the RL AGNs where exist a weak, small-scale jet (e.g., Miller et al. 1993; Falcke et al. 1996). A small fraction of RQ objects show core-jet or linear structures at pc-scale or sub-pc scale, which do support the weak-jet scenario (e.g., Ho & Ulvestad 2001; Ulvestad et al. 2005; Leipski et al. 2006). The accretion-jet model is frequently used to model the multiwavelength spectral energy distribution (SED) of AGNs (particularly in LLAGNs, e.g., Yuan et al. 2009a; Yu et al. 2011; Nemmen et al. 2012). However, this scenario cannot answer the bimodality of RL/RQ distribution for AGNs (e.g., Kellermann et al. 1994; Sikora et al. 2007). The second possibility is that the radio emission of the RQ AGNs come from the hot optically thin plasma in the disk winds, where the plasma is completely ionized and has a density high enough for bremsstrahlung emission that make a significant contribution to the observed compact radio core (e.g., Blundell & Kuncic 2006; Steenbrugge et al. 2011). In this model the mass-loss rate in the winds are significant and the observed luminosities of radio emission from quasars imply that they should accrete at super-Eddington rates. However, most of RQ AGNs are accreting at sub-Eddington rates, where the radio core emission should not dominantly come from the disk winds. The third possibility is that the radio emission also come from the accretion flows (e.g., RIAF or disk corona). Laor & Behar (2008) found that the tight correlation between the radio and X-ray luminosities in RQ QSOs is similar to that of active stars ($L_R \sim 10^{-5} L_X$). They, therefore, proposed that both the radio and X-ray emission from the nuclei of RQ AGNs may dominated by the magnetic reconnection heated corona. Wu & Cao (2005) found that

the radio emission of most nearby LLAGNs is higher than that predicted by radiation from the pure thermal electrons in the RIAF, and their radio emission should have other origin (e.g., nonthermal electrons in RIAF or jet). The radio spectrum of Sgr A*, a supermassive BH in our galaxy, consists of two components, which dominate below and above 86 GHz, respectively. Yuan et al. (2003) found that the component above 86 GHz can be well explained by the thermal electrons from the RIAF, while low-frequency radio spectrum can be explained if there exist a small fraction of nonthermal electrons in the RIAF (see also Özel et al. 2000).

It is natural that both the thermal and nonthermal electrons exist in the hot plasma (RIAF or disk corona), since that the turbulence, magnetic reconnection, and weak shocks can accelerate electrons and generate a nonthermal tail at high energies in the distribution function of thermal electrons. The Sgr A* provide an excellent observational evidence for the existence of hybrid of thermal and nonthermal electrons in accretion flows (e.g., RIAF), since that no evident radio jet was observed up to now and, therefore, its radio emission may be dominated by other mechanisms. It is interesting to note that there is also independent observational evidence for nonthermal electrons in accretion flows. McConnell et al. (2000) reported a high-energy tail in the hard state of the X-ray binary, Cygnus X-1, extending from 50 keV to ~ 5 MeV. The data at MeV energies, collected with the COMPTEL instrument of the Compton Gamma-Ray Observatory, can be explained by a power-law distribution of nonthermal electrons in the RIAF/corona (e.g., Romero et al. 2010). In this work, we try to explore whether the nonthermal electrons in RIAF can explain the radio emission of nearby LLAGNs, which always have only compact radio cores.

2. SAMPLE

To examine whether the radio emission of nearby LLAGNs with only compact cores can be explained by the nonthermal electrons in the RIAF, we search the literatures for high-resolution radio and X-ray data to ensure that their emission being from the nuclei of sources. In the radio band, we only selected the sources that have been observed by high-resolution radio telescopes (e.g., VLA, MERLIN, VLBA and VLBI), which are mainly chosen from Ho & Ulvestad (2001), Filho et al. (2006) and Nagar et al. (2005), where all these works tried to give a complete radio imaging survey of all nearby LLAGNs given in Palomar spectroscopic survey (Ho et al. 1997). For purpose of our study, we exclude the sources that observed with radio jet or even linear radio structures where the radio emission may mainly originate in the jets/outflows. The 5 GHz nuclear radio luminosities are shown in Table (1), where two sources observed at other waveband (NGC 1097 at 8.4 GHz and NGC 4736 at 15 GHz) was converted to 5 GHz by assuming $F_\nu \propto \nu^{-0.5}$ as found in Ho et al. (2001) for LLAGNs. In the X-ray waveband, we only selected the sources have compact X-ray cores, which are observed by high-resolution telescopes of *Chandra* and/or *XMM-Newton*. Several sources with the high-resolution optical data from *HST* are also included in building the SEDs (Eracleous et al. 2010, and references therein). Maoz et al. (2005) gave lower limits

TABLE 1
THE SAMPLE OF LLAGNS

Name	D_L Mpc	$\log M_{\text{BH}}$ M_{\odot}	$\log L_{5\text{GHz}}$ erg/s	Telescope	$\log L_{2-10\text{keV}}$ erg/s	Telescope	\dot{m}_{out}	η	Refs.
(1)	(2)	(3)	(4)	(5)	(6)	(7)	(8)	(9)	(10)
NGC 1097	14.5	8.10	35.98	VLA	40.63	C	1.1×10^{-3}	0.03%	1,2,3
NGC 2787	13.0	8.07	37.06	VLBA	39.28	C	3.0×10^{-4}	10.0%	4,4,5
NGC 3147	40.9	8.60	37.78	VLBA	41.88	C	5.3×10^{-3}	0.5%	4,4,6
NGC 3169	19.7	7.79	37.16	VLBA	41.41	C	6.0×10^{-3}	3.0%	4,4,6
NGC 3226	23.4	8.07	37.06	VLBA	40.74	C	1.1×10^{-3}	3.0%	4,4,6
NGC 3227	20.6	7.44	36.31	VLBA	41.70	X	2.1×10^{-2}	0.4%	4,4,7
NGC 3414	24.9	8.42	36.59	MERLIN	39.89	C	4.2×10^{-4}	0.3%	8,8,5
NGC 3718	17.0	7.85	36.77	VLBA	40.44	C	1.4×10^{-3}	3.0%	4,4,9
NGC 3941	18.9	7.55	35.69	VLA	39.27	X	5.5×10^{-4}	0.5%	10,10,7
NGC 3998	21.6	8.72	38.34	VLBA	41.79	X	2.3×10^{-3}	3.0%	4,4,11
NGC 4138	17.0	7.51	36.13	VLA	41.48	X	1.5×10^{-2}	0.1%	10,10,7
NGC 4143	17.0	8.25	37.15	VLBA	40.04	C	5.0×10^{-4}	3.0%	4,4,6
NGC 4168	16.8	7.98	36.63	VLBA	39.32	X	3.8×10^{-4}	4.0%	4,4,12
NGC 4203	9.7	7.77	36.70	VLBA	39.70	C	6.0×10^{-4}	5.0%	4,4,13
NGC 4477	16.8	8.00	35.46	VLA	39.60	X	4.95×10^{-4}	0.04%	10,10,7
NGC 4565	9.7	7.46	36.26	VLBA	39.56	C	7.0×10^{-4}	7.0%	4,4,6
NGC 4594	9.2	8.46	37.79	VLA	39.95	C	3.2×10^{-4}	15.0%	14,15,5
NGC 4639	16.8	6.68	35.57	VLA	40.18	C	4.5×10^{-3}	4.0%	10,10,13
NGC 4698	16.8	7.41	35.64	VLA	38.70	C	3.5×10^{-4}	3.0%	10,10,5
NGC 4736	4.3	6.98	35.51	VLA	38.77	C	5.7×10^{-4}	3.0%	1,4,16

Note. — Column 1: galaxy name; Column 2: galaxy distance; Column 3: BH mass; Column 4: monochromatic power at 5 GHz; Column 5: the telescope for radio data; Column 6: 2-10 keV X-ray luminosity; Column 7: the telescope for X-ray data, where 'C' denote *Chandra* and 'X' denote *XMM-Newton*; Column 8 and 9: model parameters resulting from the SED fits; Column 10: references for the distance, radio luminosity and X-ray luminosity respectively.

References: (1) Eracleous et al. (2010); (2) Thean et al. (2000); (3) Nemmen et al. (2006); (4) Nagar et al. (2005); (5) Gonzalez-Martin et al. (2009); (6) Terashima & Wilson (2003); (7) Cappi et al. (2006); (8) Filho et al. (2006); (9) Satyapal et al. (2005); (10) Ho & Ulvestad (2001); (11) Ptak et al. (2004); (12) Panessa et al. (2006); (13) Ho et al. (2001); (14) Ho (1999); (15) Hummel et al. (1984); (16) Eracleous et al. (2002).

for the intrinsic AGN optical emission for a sample of LINERs, which were constrained from their optical variabilities. We also include the lower limits of the intrinsic AGN optical emission for three sources (NGC 3998, NGC 4594 and NGC 4736, Maoz 2007). We estimate the BH mass from the velocity dispersion σ_* of the host bulges for LLAGNs in our sample using the $M_{\text{BH}} - \sigma_*$ relation given by Tremaine et al. (2002). Most of velocity dispersions are selected from the Hyperleda database² with one exception, NGC 1097, from Eracleous et al. (2010). We find that the velocity dispersion of most LLAGNs in our sample is consistent with that reported in Ho et al. (2009). Our sample include 20 LLAGNs (see Table 1).

3. MODEL

In this work, we consider the RIAF model proposed by Yuan et al. (2003), which can be considered as an updated version of the original ADAF (e.g., Narayan & Yi 1995), where both outflows and the possible existence of nonthermal electrons are considered. Here, we briefly summarize the model as follows.

The more accurate global structure and dynamics of the accretion flow is calculated numerically to obtain the ion and electron temperature, density at each radius. In particular, we employ the approach suggested by Manmoto (2000) for calculating the structure of the RIAF in general relativistic frame, which allows us to calculate the structure of the accretion flow surround-

ing either a spinning or a nonspinning BH. In this work, we calculate the global structure of the accretion flows surrounding massive Schwarzschild black holes. In stead of using a constant accretion rate, we assume that the accretion rate is a function of radius, e.g., $\dot{M} = \dot{M}_{\text{out}}(R/R_{\text{out}})^s$ (e.g., Blandford & Begelman 1999; Stone et al. 1999; Igumenshchev & Abramowicz 1999; Stone & Pringle 2001; Li & Cao 2009; Yuan & Bu 2010), where R_{out} is the outer radius of the RIAF and \dot{M}_{out} is the accretion rate at R_{out} . The global structure of the RIAF can be calculated with proper outer boundaries, if the parameters \dot{m} , α , β , and δ are specified (see Manmoto 2000, for more details). All radiation processes (synchrotron, bremsstrahlung and Compton scattering) are included self-consistently in the calculations of the RIAF structure. The parameter $\dot{m} = \dot{M}/\dot{M}_{\text{Edd}}$ is dimensionless accretion rate, where the Eddington accretion rate is defined as $\dot{M}_{\text{Edd}} = 1.4 \times 10^{18} M_{\text{BH}}/M_{\odot} \text{ gs}^{-1}$. For the viscosity parameter α and magnetic parameter $\beta = P_{\text{g}}/P_{\text{tot}}$ [defined as the ratio of the gas to the total pressure (sum of gas and magnetic pressure)], we adopt typical values of $\alpha = 0.3$ and $\beta = 0.9$, which are widely used in RIAF models. There is obviously a degeneracy between \dot{m}_{out} and s when the accretion rate at the innermost region of the RIAF is concerned. We adopt $s = 0.3$ in this work, which is well constrained from the observation of our Galactic center black hole, Sgr A* (Yuan et al. 2003, but see also

² <http://leda.univ-lyon1.fr>

Yuan et al. (2012) for slightly higher value of $s \sim 0.4 - 0.5$ from simulations). We fix the outer boundary at $5000R_g$ ($R_g = GM_{\text{BH}}/c^2$ is gravitational radius), which is roughly consistent with the prediction of the disk-corona evaporation model for the LLAGNs with very low Eddington ratios (e.g., $10^{-7} \lesssim L_{2-10 \text{ keV}}/L_{\text{Edd}} \lesssim 10^{-4}$, Liu & Taam 2009). The most poorly constrained parameter is δ , which describes the fraction of the turbulent dissipation that directly heats the electrons in the flow. Sharma et al. (2007) found that the parameter δ may be in range of $\sim 0.01 - 0.3$ based on the simulations, depending on the model details. In this work, we adopt $\delta = 0.1$ because we find that the X-ray spectra of most LLAGNs in our sample can be well fitted with this fixed δ value.

Following Yuan et al. (2003), we assume that the injected energy in the nonthermal electrons is equal to a fraction η of the energy in thermal electrons, where we take η to be independent of the radius. The thermal electrons are assumed to have relativistic Maxwell-Boltzmann distribution, while the nonthermal electrons are assumed to be the power-law tail of the thermal electrons, which can be described by the parameter p [$n(\gamma) \propto \gamma^{-p}$, where γ is the electron Lorentz factor]. The number density of the nonthermal electrons can be obtained if η is given. Özel et al. (2000) proposed that the parameters, p and η , for describing the nonthermal electrons are degenerate in the radio waveband in our model. Therefore, we adopt a fiducial value of $p = 3.0$, and allow the parameter η to be free.

After determining the distribution of thermal and nonthermal electrons, we calculate their radiation. The synchrotron emission from both thermal and nonthermal electrons are calculated (e.g., Yuan et al. 2003). The Comptonization of seed photons from both thermal and nonthermal electrons are considered, which was calculated by the method proposed by Coppi & Blandford (1990). In spectral calculations, the gravitational redshift effect is considered, while the relativistic optics near the black hole is neglected. More details about spectrum calculation can be found in Yuan et al. (2003, and references therein).

In summary, our model have only two free parameters, \dot{m}_{out} and η in fitting the SED of LLAGNs.

4. RESULTS

We present the typical spectrum of the RIAF with a population of hybrid electrons in Figure 1 (top panel), where the short-dashed, long-dashed and solid lines represent the emission from the thermal electrons, nonthermal electrons and sum of them respectively, where typical parameters $M_{\text{BH}} = 10^8 M_{\odot}$, $\dot{m}_{\text{out}} = 10^{-3}$, and $\eta = 1\%$ are adopted for given outer radius $R_{\text{out}} = 5000R_g$. In this model, the X-ray emission mainly come from the Comptonization of seed photons that produced by both thermal electrons and nonthermal electrons. We find that the low-frequency radio emission is dominated by the self-absorbed synchrotron emission from the nonthermal electrons, which is normally 2-3 order of magnitude higher than that from thermal electrons in RIAF. Our results are similar for other parameters if the typical parameter $\eta \sim$ several percent is adopted as that used in Sgr A* (Yuan et al. 2003, 2006). The high-energy X-ray emission dominantly come from the inner region of the accretion

flows (e.g., within several tens gravitational radii). However, we find the region of the radio emission is much larger. The dotted lines in Figure 1 (top panel) show the spectrum from the nonthermal electrons with outer boundary $R_{\text{out}} = 3000R_g$, $1000R_g$ and $500R_g$ respectively for above given other parameters. We find that the radiation region of the low-frequency radio emission at several GHz can up to several thousands gravitational radii, where the radio emission at $\gtrsim 3000R_g$ is negligible. The bottom panel of Figure 1 show the spectrum of nonthermal electrons with $p = 2.5$, $\eta = 0.5\%$ (solid line); $p = 3.0$, $\eta = 1\%$ (dashed line) and $p = 3.5$, $\eta = 5\%$ (dotted line), where the other parameters keep the same as above. It can be found that p and η are degenerate for radio emission (e.g., $\lesssim 10$ GHz, see also Özel et al. 2000). Therefore, it should be impossible to determine p and η from the observational low-frequency radio emission alone.

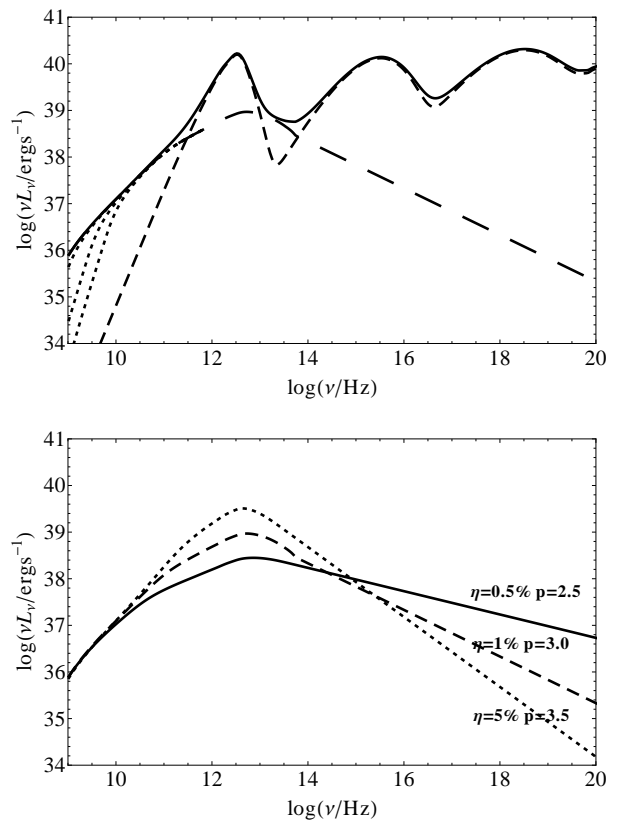


FIG. 1.— The top panel show the typical spectrum of the RIAF with both thermal and nonthermal electrons for $M_{\text{BH}} = 10^8 M_{\odot}$, $\dot{m}_{\text{out}} = 10^{-3}$, $\eta = 1\%$ and $p = 3.0$ at given $R_{\text{out}} = 5000R_g$, where the short-dashed, long-dashed and solid lines are the radiation from the thermal electrons, nonthermal electrons and sum of them respectively. The dotted lines represent the radiation of the nonthermal electrons in the RIAF with different outer radius at $3000R_g$, $1000R_g$, and $500R_g$ (from top to bottom) respectively. The bottom panel show the spectrum from the nonthermal electrons with $p = 2.5$, $\eta = 0.5\%$ (solid line); $p = 3.0$, $\eta = 1\%$ (dashed line), and $p = 3.5$, $\eta = 5\%$ (dotted line) respectively, where the other parameters are the same as above.

Our calculations show that the X-ray emission from the RIAF is almost proportional to the BH mass for a given \dot{m} , and it scales as \dot{m}^q with $q \simeq 2$ for a given BH mass (see also Wu & Cao 2006; Merloni et al. 2003). In this work, we

further explore the possible relation between the radio luminosity and BH mass/accretion rate for RIAF model with both thermal and nonthermal electrons, where the radio emission dominantly originate in the nonthermal electrons. Figure 2 (top panel) shows the relation between radio luminosity and BH mass for $\dot{m}_{\text{out}} = 10^{-2}$ and $\dot{m}_{\text{out}} = 10^{-4}$ with $\eta = 1\%$ respectively, where we find that the radio emission is roughly proportional to $M_{\text{BH}}^{1.4}$ (solid lines). The bottom panel of Figure 2 shows the relation between the radio luminosity and dimensionless accretion rate for given BH masses $M_{\text{BH}} = 10^7$ and $10^9 M_{\odot}$ respectively, where we find that the radio emission is roughly proportional to \dot{m}^{ξ} with $\xi \simeq 0.8$ for both cases. To explore the radio emission for a sample of LLAGNs with different BH masses as a whole, we define a mass-corrected radio-loudness as $R_{\text{M}} = R_{\text{X}}/M_{\text{BH}}^{0.4}$, according to the dependence of the radio and X-ray emission on the BH mass in our model, where $R_{\text{X}} = L_{5\text{GHz}}/L_{2-10\text{keV}}$.

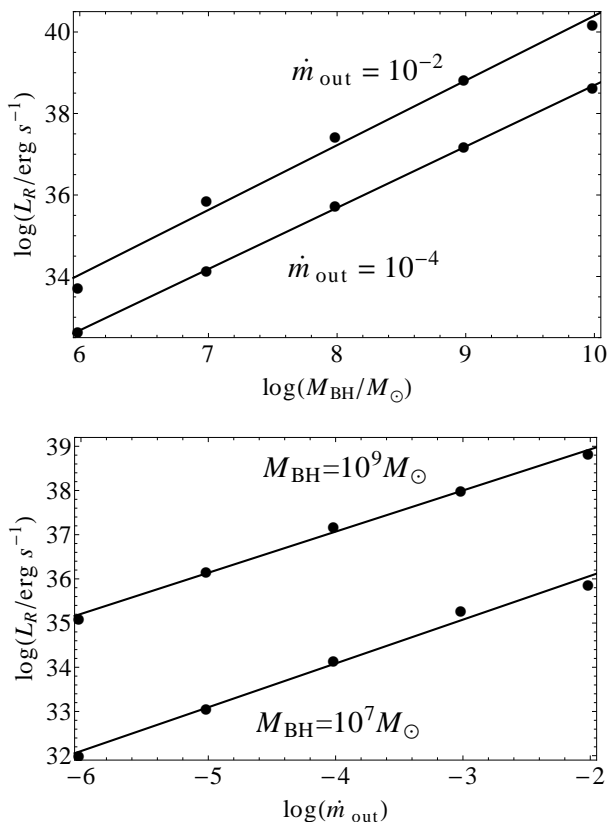


FIG. 2.— Top panel show the model prediction on the relation between $L_{5\text{GHz}}$ and M_{BH} for two given accretion rates $\dot{m}_{\text{out}} = 10^{-2}$ and $\dot{m}_{\text{out}} = 10^{-4}$ with $\eta = 1\%$, where the solid points represent $M_{\text{BH}} = 10^6, 10^7, 10^8, 10^9$, and $10^{10} M_{\odot}$ respectively, and the solid lines are their best fittings. The bottom panel present the relation between $L_{5\text{GHz}}$ and \dot{m}_{out} for two given BH masses $M_{\text{BH}} = 10^7$ and $M_{\text{BH}} = 10^9 M_{\odot}$, where the solid points represent $\dot{m}_{\text{out}} = 10^{-6}, 10^{-5}, 10^{-4}, 10^{-3}$, and 10^{-2} respectively, and solid lines are their best fittings.

We present the relation between the mass-corrected loudness, R_{M} , and the Eddington ratio, $L_{2-10\text{keV}}/L_{\text{Edd}}$, for all LLAGNs in Figure 3, where both quantities roughly do not depend on the BH mass. It can be found that there

is an anti-correlation between R_{M} and $L_{2-10\text{keV}}/L_{\text{Edd}}$ for LLAGNs. We further demonstrate the theoretical relation between R_{M} and $L_{2-10\text{keV}}/L_{\text{Edd}}$ in our model for different values of η from 0 to 10% at given $M_{\text{BH}} = 10^8 M_{\odot}$ (see Figure 3). It can be found that our theoretical model also predict that R_{M} is anti-correlate with $L_{2-10\text{keV}}/L_{\text{Edd}}$ as observational features of LLAGNs. This is because the loudness R_{M} of our model scales $R_{\text{M}} \propto L_{\text{R}}/L_{\text{X}} \propto \dot{m}^{-1.2}$, while $L_{\text{X}}/L_{\text{Edd}} \propto \dot{m}^2$. We find that the radio emission of most LLAGNs can be explained by our model if $\sim 0.01 - 10\%$ of the electron energy is ejected into the nonthermal electrons (see Figure 3). However, pure RIAF without power-law electrons ($\eta = 0$, see Figure 3) always underpredicts the radio emission by several orders of magnitude compared the observations.

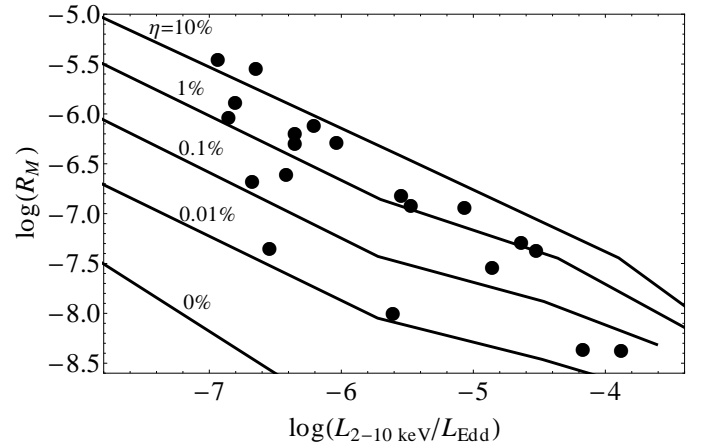


FIG. 3.— The relation between the mass-corrected radio loudness, $R_{\text{M}} = R_{\text{X}}/M_{\text{BH}}^{0.4}$, and the Eddington-scaled X-ray luminosity, $L_{2-10\text{keV}}/L_{\text{Edd}}$, where $R_{\text{X}} = L_{5\text{GHz}}/L_{2-10\text{keV}}$. The solid points represent the LLAGNs in our sample, and the solid lines represent the model prediction with the parameter $\eta = 10\%, 1\%, 0.1\%, 0.01\%$, and 0% (from top to bottom) respectively.

We further fit the radio to X-ray spectrum of all sources in our sample using the RIAF model with hybrid electrons. The results are shown in Figures 4-5, and the adopted parameters, \dot{m}_{out} and η , of each source are listed in Table (1). With exception of the optical/UV waveband in several sources, the model can successfully fit the SED of these sources from the radio to hard X-rays with only two free parameters. The X-ray emission dominantly come from the thermal electrons of the RIAF for all sources in our sample, while the observed radio emission is always 2-3 orders of magnitude higher than that predicted by the purely thermal RIAF model. The radio emission can be well described by the synchrotron radiation from the nonthermal electrons in the RIAF if a small fraction of the electron thermal energy resides in the power-law tail, where the η range from 0.03% to 15%, with a typical value of $\sim 3\%$, for the sources in our present sample (see Table 1).

5. SUMMARY AND DISCUSSION

In this work, we explore the hybrid thermal-nonthermal synchrotron emission from the hot accretion-flows of the RIAF. Such hot accretion flows are expected to exist in sources with low-mass accretion rates (e.g., LLAGNs). We

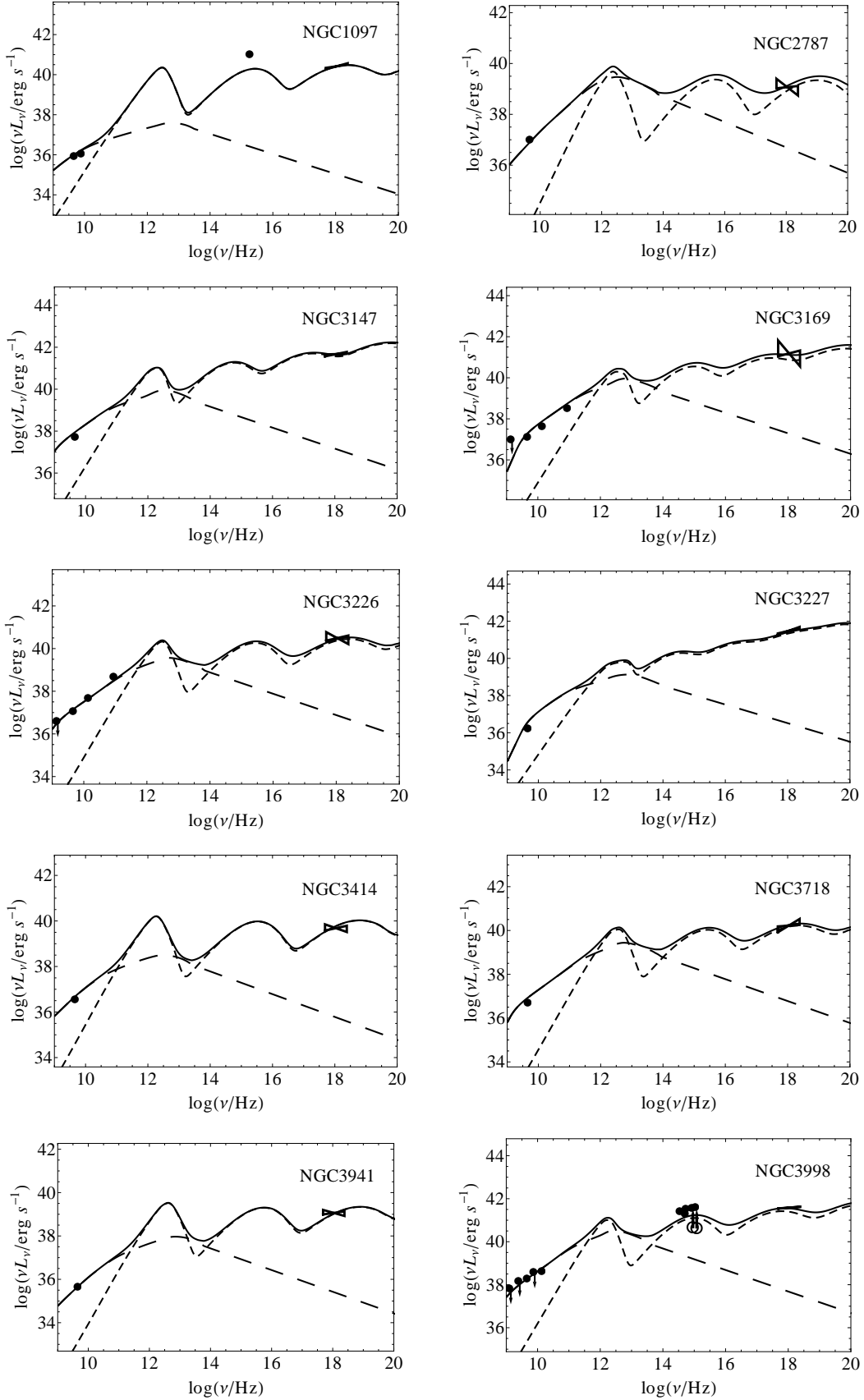


FIG. 4.— Models for the SED of LLAGNs. The solid points represent the observed emission, and the empty circles denote the lower limit for the intrinsic AGN optical emission that derived from the variability of optical emission. The short-dashed and long-dashed lines represent the emission from the thermal and nonthermal electrons of the RIAF respectively, while the solid line show the radiation from both of these two components.

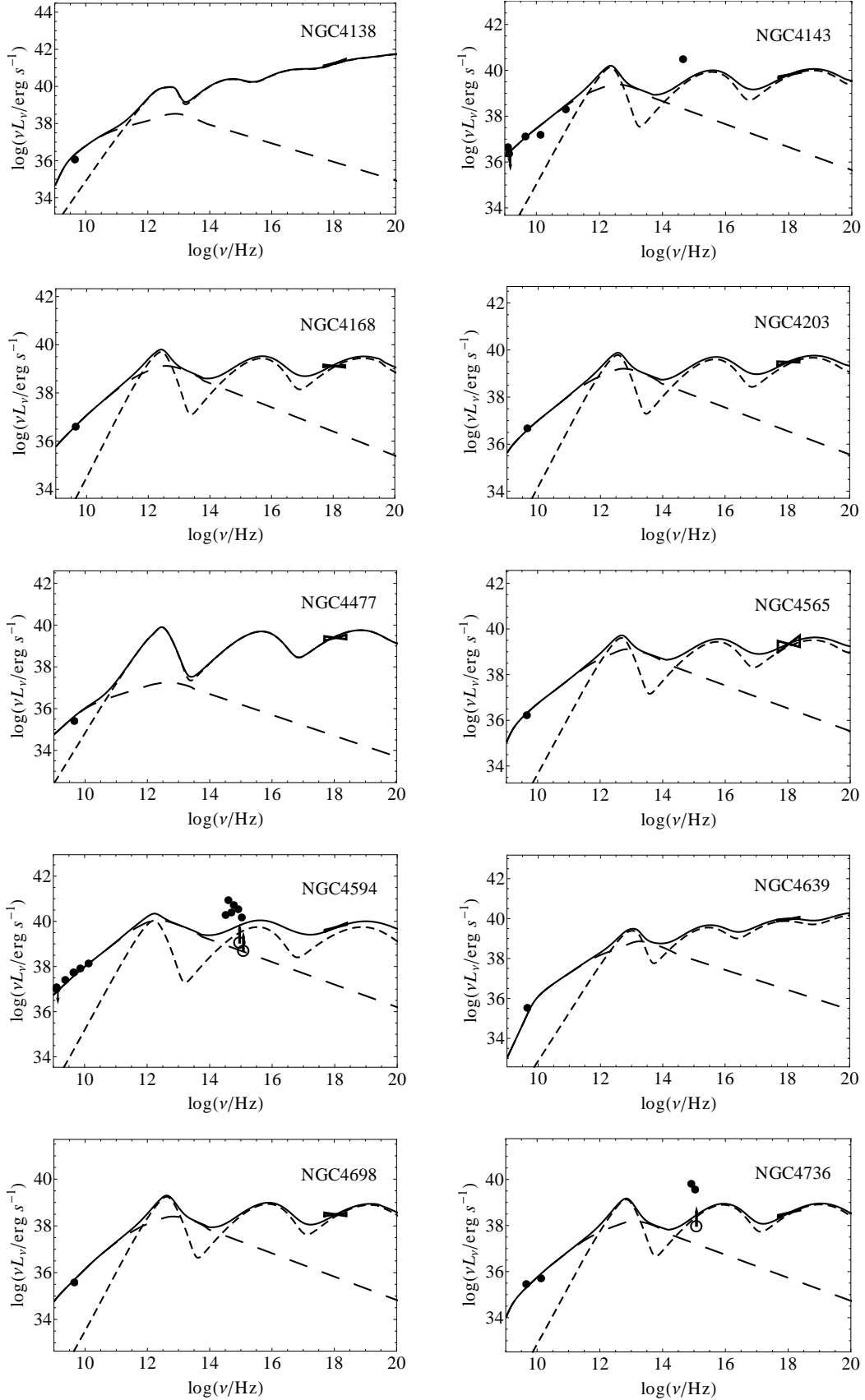


FIG. 5.— The same as Figure 4, but for the remaining 10 LLAGNs.

calculate the spectrum of the global RIAF model with hybrid electrons, and find that synchrotron emission from the nonthermal electrons can be up to 2-3 orders of magnitude greater than that from the purely thermal electrons even with only several percent of electron thermal energy injected into the nonthermal electrons. This model has explained the multi-wavelength spectrum of Sgr A* very well (Yuan et al. 2003), and we further extend this model to other nearby LLAGNs, which have only a compact radio core and have no evidence of the jet. Our model can roughly reproduce the observed anticorrelation between the mass-corrected radio loudness and Eddington ratio as found in the LLAGNs. We further perform the detailed modeling of the SED for 20 LLAGNs in our sample from the radio to X-ray waveband. We find that the SED of LLAGNs can be well described by our model, where the X-ray emission is produced predominantly by the inverse Compton scattering of the seed synchrotron photons produced by both thermal and nonthermal electrons in the RIAF, while the radio emission mainly come from the nonthermal electrons.

It is now established that RQ AGNs are not radio-silent, and do emit the radio emission at some level. Ho & Ulvestad (2001) found that 85% of the nearby Seyfert nuclei show the nuclear radio emission at 5 GHz, and their typical radio morphology is a compact core (either unresolved or slightly resolved). Anderson et al. (2004) observed six nearby LLAGNs with high-resolution VLBA, and found that the radio emission is still unresolved even at milliarcsecond scale, which roughly corresponds to several to ten thousands gravitational radii. Therefore, contrary to the RL AGNs which have been observed with jet or core-jet structures directly, the physical origin of the radio emission in RQ AGNs is much unclear. The most popular model is that there may exist a scaled-down version of the jet in RQ AGNs. The coupled RIAF-jet model has been explored to fit the multi-wavelength spectrum of LLAGNs (e.g., Wu et al. 2007; Yuan et al. 2009a; Yu et al. 2011; Nemmen et al. 2012). We note that it is reasonable to apply the RIAF-jet model to the sources with observed jet structures (e.g., FR Is), while it is still controversial whether the same model can be used to the LLAGNs with only compact radio cores, where these sources have no evident jet structure even at scale of several thousand gravitational radii. Another possibility is that the radio emission in RQ AGNs also originate in the hot plasma (e.g., RIAF in LLAGNs and disk-corona in bright AGNs), where the turbulence, weak shocks and/or magnetic reconnection events may occasionally accelerate a fraction of the electrons to a harder power-law tail. The synchrotron emission from these nonthermal power-law electrons may account for the radio emission from the compact cores of these LLAGNs. The hybrid thermal-nonthermal synchrotron emission from the RIAF have well reproduced the two components of the radio spectrum and also the X-ray flares observed in Sgr A* (e.g., Yuan et al. 2003). We confirm the result that the pure RIAF always underpredicts the radio emission for nearby LLAGNs (Wu & Cao 2005). However, the low-frequency radio emission of the compact cores in LLAGNs can be accounted if only a small fraction of the viscous dissipation energy in the accretion flow goes into accelerating electrons

to a nonthermal power-law distribution (see Figures 4-5). It is well established that magnetic reconnection should be unavoidable and play an important role in converting the magnetic energy into the particles (e.g., Hawley & Balbus 2002; Goodman & Uzdensky 2008). Both the magnetic reconnection itself (e.g., Ding et al. 2010) or the diffusive shock caused by the violent plasma motions in the magnetic reconnection region (e.g., Spruit 1988) can naturally accelerate a small fraction of the electrons to be the power-law distribution. A small fraction of the power-law electrons presented in the RIAF will not affect the global structure of the RIAF (e.g., Özel et al. 2000). Therefore, our work provide the possibility that the radio emission of nearby LLAGNs may originate in the nonthermal electrons of the hot accretion flow. It may be the similar case for other bright RQ AGNs, where the radio emission is dominated by the nonthermal electrons in the corona. Laor & Behar (2008) found the similarities of the radio/hard X-ray correlation in RQ AGNs and magnetically active stars, which support that the radio emission of RQ AGNs also dominantly come from the corona as that of active stars. We will further test this issue in a subsequent work for bright RQ AGNs considering the possible physical mechanism for the production of thermal and nonthermal electrons in the corona above the SSD.

Ho (2002) found a strong anticorrelation between the radio loudness and Eddington ratio for the LLAGNs (see also Sikora et al. 2007; Panessa et al. 2007; Younes et al. 2012). We investigate the dependence of the mass-corrected radio loudness, $R_M = R_X/M_{\text{BH}}^{0.4}$, on the Eddington ratio, $L_{2-10\text{keV}}/L_{\text{Edd}}$, where the scaling of $M_{\text{BH}}^{0.4}$ is derived from our model as that $L_X \propto M_{\text{BH}}$ and $L_R \propto M_{\text{BH}}^{1.4}$. We find that the mass-corrected radio loudness is still anticorrelate with the Eddington ratio, where both quantities are not affected by the mass term. It is interesting to note that the dependence of the radio emission on the BH mass, $L_R \propto M_{\text{BH}}^{1.4}$, in our model is similar to that of jet model (e.g., Heinz & Sunyaev 2003) and that derived from the observed fundamental plane of BH activity (Merloni et al. 2003; Falcke et al. 2004). Therefore, it should be cautious to get the conclusion that the origin of the radio and X-ray emission is similar for the stellar-mass BH X-ray binaries (XRBs) and the supermassive BH AGNs based only on the fundamental plane equation of the BH activity, since that the dependence of the radio emission on the BH mass is similar for our model and the jet model. We find that the relation between the radio luminosity and X-ray luminosity is $L_R \propto L_X^{0.4}$ at a given BH mass in our model based on $L_R \propto \dot{m}^{0.8}$ and $L_X \propto \dot{m}^{2.0}$. Our model prediction on the radio-X-ray correlation is much shallower than that observed in XRBs (e.g., Gallo et al. 2003; Corbel et al. 2003) or that predicted by accretion-jet model (e.g., Yuan & Cui 2005), where $L_R \propto L_X^{0.7}$. Our results provide a diagnostic that can distinguish the possible origin of the radio emission in LLAGNs by investigating the radio-X-ray correlation for LLAGNs with the same or similar BH masses. However, our present sample is still limited, which prevent us to further test this issue.

From a theoretical perspective, there are still some uncertainties in the current RIAF model with hybrid thermal and nonthermal electrons. The dependence of the spectrum on the model parameters have been explored in

former works (e.g., Quataert & Narayan 1999; Özel et al. 2000). The RIAF spectrum is not sensitive to some parameters (e.g., α , β), we adopt the typical values $\alpha = 0.3$ and $\beta = 0.9$, which are constrained from observations and/or simulations. Wind parameter $s = 0.3$ is adopted directly, which is constrained from observations of Sgr A*. We adopt the radius $R_{\text{out}} = 5000R_g$ as the outer boundary. We find that the X-ray emission mainly come from the innermost region of the accretion flow, which is less affected by the outer boundary condition if it is larger than several tens gravitational radii. However, we find that the low-frequency radio emission come from the much larger regions from several tens to several thousand gravitational radii. The LLAGNs in our sample have very low Eddington ratios ($10^{-7} \lesssim L_{2-10 \text{ keV}}/L_{\text{Edd}} \lesssim 10^{-4}$), and the whole accretion may be through RIAF. Liu & Taam (2009) proposed that the truncation radius should be around one thousand to several tens of thousands gravitational radii (if the possible outer SSD is present) for $\dot{m} \sim 10^{-4} - 10^{-2}$ as adopted in fitting the SED of the LLAGNs in our sample. Therefore, the assumption of the outer boundary $R_{\text{out}} = 5000R_g$ should be reasonable, and will not affect our main results. The region of the radio emission from the nonthermal electrons in RIAF is more or less consistent with the size of the compact radio cores as observed by the VLBI for some nearby LLAGNs (e.g., Wrobel & Ho 2006). We neglect the contribution of the emission from the possible outer SSD (if present) in our SED fittings, since that we still don't know whether the outer SSD still exists in the LLAGNs with extreme low Eddington ratios or not, and the optical emission also easily suffer the contamination from the host galaxies or contaminate by the nuclear starbursts. For example, Storchi-Bergmann et al. (2005) reported an evidence of recent starburst formation in the nucleus of NGC 1097, and its optical/UV emission may dominated by the stellar contribution. We find that our model prediction on the optical emission is slightly smaller than the observed emission but higher than the lower limits of the possible intrinsic AGN optical emission that derived from optical variabilities. Therefore, the observed optical emission of

LLAGNs is roughly consistent with our model predictions even without considering the possible contribution from the outer SSD (e.g., Figures 4-5). The parameter δ , describing the fraction of the turbulent dissipation that directly heats the electrons in the flow, is still unclear, which may be in the range of several percent up to several tens percent based on recent simulations (e.g., Sharma et al. 2007) and/or model fitting of the Sgr A* (Yuan et al. 2003, 2006). We find that most of LLAGNs in our sample can be better fitted if $\delta = 0.1$ is adopted (see Figures 4-5). It should be noted that the adopted $\delta = 0.1$ is slightly smaller than that used in Sgr A* ($\delta = 0.3$, Yuan et al. 2003), which may caused by different microphysics since that the accretion rate in Sgr A* much smaller than that used in our work. Our results will be roughly unchanged even if we use $\delta = 0.3$ as that used in Sgr A* (e.g., Yuan et al. 2006), but the model fitting of the X-ray emission is less perfect as that with $\delta = 0.1$. The values of p and η that describing the nonthermal electrons is not strongly constrained, but which are degenerate for low-frequency radio emission (e.g., Özel et al. 2000). We fix the typical value of $p=3.0$, and then adjust the parameter η to fit the radio emission of LLAGNs in our sample. We find that only a small fraction of the energy in nonthermal electrons is sufficient to produce the radio emission at low frequencies. The value of η can even be smaller if the parameter p is also smaller. Our fitting results show that the value of η in these LLAGNs of our sample is more or less consistent with that constrained for Sgr A* (e.g., $\sim 1\%$ in Yuan et al. 2003, 2006) and that derived from the gamma-ray background (e.g., $\sim 4\%$ in Inoue et al. 2008).

We appreciate Feng Yuan, Xinwu Cao and the anonymous referee for helpful comments and suggestions. We also thank the members of HUST astrophysics group for useful discussions. This work is supported by the National Basic Research Program of China (2009CB824800), the NSFC (grants 11103003, 11133005 and 11173011), the Doctoral Program of Higher Education (20110142120037), the Fundamental Research Funds for the Central Universities (HUST: 2011TS159).

REFERENCES

- Abramowicz, M. A., Chen, X., Kato, S., Lasota, J.-P., & Regev, O. 1995, *ApJ*, 438, 37
 Anderson, J. M., Ulvestad, J. S., & Ho, L. C. 2004, *ApJ*, 603, 42
 Barvainis, R., Lehar, J., Birkinshaw, M., Falcke, H., & Blundell, K. M. 2005, *ApJ*, 618, 108
 Blandford, R. D., & Begelman, M. C. 1999, *MNRAS*, 303, L1
 Blundell, K. M., & Kuncic, Z. 2006, *ApJ*, 668, 103
 Cao, X. 2010, *ApJ*, 724, 855
 Cao, X., & Rawlings, S. 2004, *MNRAS*, 349, 1419
 Cappi, M. et al. 2006, *A&A*, 446, 459
 Coppi, P. S., & Blandford, R. D. 1990, *MNRAS*, 245, 453
 Ding, J. Yuan, F., & Liang, E. 2010, *ApJ*, 708, 1545
 Eracleous, M., Shields, J. C., Chartas, G., & Moran, E. C. 2002, *ApJ*, 565, 108
 Eracleous, M., Hwang, J. A., Flohic, & H. M. L. G. 2010, *ApJS*, 187, 135
 Falcke, H., K rding, E. G., & Markoff, S. 2004, *A&A*, 414, 895
 Falcke, H., & Markoff, S. 2000, *A&A*, 362, 113
 Falcke H., Sherwood W., & Patnaik A. R., 1996, *ApJ*, 471, 106
 Filho, M. E., Barthel, P. D., & Ho, L. C. 2006, *A&A*, 451, 71
 Corbel, S., Nowak, M. A., Fender, R. P., Tzioumis, A. K., & Markoff, S. 2003, *A&A*, 400, 1007
 Gallo, E., Fender, R. P., & Pooley, G. G. 2003, *MNRAS*, 344, 60
 Gebhardt K., et al. 2000, *ApJ*, 543, 5
 Giroletti, M., & Panessa, F. 2009, *ApJ*, 706, 260
 Goodman, J., & Uzdensky, D. 2008, *ApJ*, 688, 555
 Gonzalez-Martin, O., Masegosa, J., Marquez, I., Guainazzi, M., & Jimenez-Bailon, E. 2009, *A&A*, 506, 1107
 Gu, M., & Cao, X. 2009, *MNRAS*, 399, 349
 Hawley, J. F., & Balbus, S. A. 2002, *ApJ*, 573, 738
 Heinz, S., & Sunyaev, R. A. 2003, *MNRAS*, 343, 59
 Ho, L. C., Greene, J. E., Filippenko, A. V., Sargent, W. L. W. 2009, *ApJS*, 183, 1
 Ho, L. C. 2009, *ApJ*, 699, 626
 Ho, L. C. 2008, *ARA&A*, 46, 475
 Ho, L. C. 2002, *ApJ*, 564, 120
 Ho, L. C., et al. 2001, *ApJ*, 549, 51
 Ho, L. C., & Ulvestad, J. S. 2001, *ApJS*, 133, 77
 Ho, L. C. 1999, *ApJ*, 516, 672
 Ho, L. C., Filippenko, A. V., & Sargent, W. L. W. 1997, *ApJ*, 487, 568
 Hopkins, P. F., & Hernquist, L. 2006, *ApJ*, 166, 1
 Hummel, E., van der Hulst, J. M., Dickey, J. M. 1984, *A&A*, 134, 207
 Ichimaru, S. 1977, *ApJ*, 214, 840
 Igumenshchev, I. V., & Abramowicz, M. A. 1999, *MNRAS*, 303, 309
 Inoue, Y., Totani, T., & Ueda, Y. 2008, *ApJ*, 672, 51
 Kaspi, S., Maoz, D., Netzer, H., Peterson, B. M., Vestergaard, M., & Jannuzi, B. T. 2005, *ApJ*, 629, 61

- Kato, S., Fukue, J., & Mineshige, S. 2008, *Black-Hole Accretion Disks: Towards a New Paradigm* (Kyoto: Kyoto Univ. Press)
- Kellermann, K. I., Sramek, R. A., Schmidt, M., Green, R. F., & Shaffer, D. B. 1994, *AJ*, 108, 1163
- Laor, A., & Behar, E. 2008, *MNRAS*, 390, 847
- Leipski, C., Falcke, H., Bannert, N., & Huttemeister, S. 2006, *A&A*, 455, 161
- Li, S.-L., Cao, X. 2009, *MNRAS*, 400, 1743
- Liu, B. F., & Taam, R. E. 2009, *ApJ*, 707, 233
- Maoz, D. 2007, *MNRAS*, 377, 1696
- Maoz, D., Nagar, N. M., Falcke, H., Wilson, A. S. 2005, *ApJ*, 625, 699
- Manmoto, T. 2000, *ApJ*, 534, 734
- McConnell, M. L., et al. 2000, *ApJ*, 543, 928
- Merloni, A., Heinz, S., & di Matteo, T. 2003, *MNRAS*, 345, 1057
- Miller P., Rawlings S., & Saunders R., 1993, *MNRAS*, 263, 425
- Nagar, N. M., Falcke, H., & Wilson, A. S. 2005, *A&A*, 435, 521
- Nagar, N. M., Falcke, H., Wilson, A. S., & Ulvestad, J. S. 2002, *A&A*, 392, 53
- Narayan, R. & McClintock, J. E. 2008, *New Astronomy Reviews*, 51, 733
- Narayan, R., & Yi, I. 1995, *ApJ*, 452, 710
- Narayan, R., & Yi, I. 1994, *ApJ*, 428, 13
- Nemmen, R., Storchi-Bergmann, T., & Eracleous, M. 2012, submitted to *ApJ*, arXiv:1112.4640
- Nemmen, R. S., Storchi-Bergmann, T., Yuan, F., Eracleous, M., Terashima, Y., & Wilson, A. S. 2006, *ApJ*, 643, 652
- Özel, F., Psaltis, D., & Narayan, R. 2000, *ApJ*, 541, 234
- Panessa, F., Barcons, X., Bassani, L., Cappi, M., Carrera, F. J., Ho, L. C., & Pellegrini, S. 2007, *A&A*, 467, 519
- Panessa, F., Bassani, L., Cappi, M., Dadina, M., Barcons, X., Carrera, F. J., Ho, L. C., & Iwasawa, K. 2006, *A&A*, 455, 173
- Ptak, A., Terashima, Y., Ho, L. C., & Quataert, E. 2004, *ApJ*, 606, 173
- Quataert, E., Di Matteo, T., Narayan, R., & Ho, L. C. 1999, *ApJ*, 525, 89
- Quataert, E., & Narayan, R. 1999, *ApJ*, 520, 298
- Romero, G. E., Vieyro, F. L., & Vila, G. S. 2010, 519, 109
- Shakura, N. I., & Sunyaev, R. A. 1973, *A&A*, 24, 337
- Sharma, P., et al. 2007, *ApJ*, 667, 714
- Sikora, M., Stawarz, L., & Lasota, J.-P. 2007, *ApJ*, 658, 815
- Spruit, H. C. 1988, *A&A*, 194, 319
- Satyapal, S., Dudik, R. P., O'Halloran, B., & Gliozzi, M. 2005, *ApJ*, 633, 86
- Stone, J. M., Pringle, J. E., & Begelman, M. C. 1999, *MNRAS*, 310, 1002
- Stone, J. M., & Pringle, J. E. 2001, *MNRAS*, 322, 461
- Steenbrugge, K. C., Jolley, E. J. D., Kuncic, Z., & Blundell, K. M. 2011, *MNRAS*, 413, 1735
- Storchi-Bergmann, T., Nemmen, R. S., Spinelli, P. F., Eracleous, M., Wilson, A. S., Filippenko, A. V., Livio, M. 2005, *ApJ*, 624, 13
- Terashima, Y. & Wilson, A. S. 2003, *ApJ*, 583, 145
- Thean, A., Pedlar, A., Kukula, M. J., Baum, S. A., & O'Dea, C. P. 2000, *MNRAS*, 314, 573
- Tremaine, S., et al. 2002, *ApJ*, 574, 740
- Ulvestad, J. S., Wong, D. S., Taylor, G. B., Gallimore, J. F., & Mundell, C. G. 2005, *ApJ*, 130, 936
- Wrobel, J. M. & Ho, L. C. 2006, *ApJ*, 646, 95
- Wu, Q. & Gu, M. 2008, *ApJ*, 682, 212
- Wu, Q., Yuan, F., & Cao, X. 2007, *ApJ*, 669, 96
- Wu, Q., & Cao, X. 2006, *PASP*, 118, 1098
- Wu, Q., & Cao, X. 2005, *ApJ*, 621, 130
- Xu, Y.-D. & Cao, X. 2009, *RAA*, 9, 401
- Younes, G., Porquet, D., Sabra, B., Reeves, J. N., & Grosso, N. 2012, *A&A*, 1039, 534
- Yu, Z., Yuan, F. & Ho, L. C. 2011, *ApJ*, 726, 87
- Yuan, F., & Narayan, R. 2013, *ARA&A*, in preparation
- Yuan, F., Wu, M., Bu, D. 2012, submitted to *ApJ*
- Yuan, F., Bu, D.-F. 2010, *MNRAS*, 408, 1051
- Yuan, F., Yu, Z., & Ho, L. C. 2009a, *ApJ*, 703, 1034
- Yuan, F. 2007, *ASP Conf. Ser.* 373, *The Central Engine of Active Galactic Nuclei*, ed. L. C. Ho and J.-M. Wang (San Francisco), 95
- Yuan, F., Shen, Z.-Q., & Huang, L. 2006, *ApJ*, 642, 45
- Yuan, F., & Cui W. 2005, *ApJ*, 629, 408
- Yuan, F., Quataert, E., & Narayan, R. 2003, *ApJ*, 598, 301
- Yuan, Y.-F., Cao, X., Huang, L., & Shen, Z.-Q. 2009b, *ApJ*, 699, 722